Journal of ELECTRONIC MATERIALS
DOI: 10.1007/s11664-017-5338-7

Cu-Induced Dielectric Breakdown of Porous Low-Dielectric-Constant Film

YI-LUNG CHENG,[1,7] CHIH-YEN LEE,[1] YAO-LIANG HUANG,[1] CHUNG-REN SUN,[2] WEN-HSI LEE,[2] GIIN-SHAN CHEN,[3] JAU-SHIUNG FANG,[4] and BACH THANG PHAN[5,6,8]

1.—Department of Electrical Engineering, National Chi-Nan University, Nan-Tou, Taiwan, ROC. 2.—Department of Electrical Engineering, National Cheng-Kung University, T'ainan, Taiwan, ROC. 3.—Department of Materials Science, Feng-Chia University, Taichung, Taiwan, ROC. 4.—Department of Materials Science and Engineering, National Formosa University, Huwei, Taiwan, ROC. 5.—Faculty of Materials Science and Laboratory of Advanced Materials, University of Science, Vietnam National University, Ho Chi Minh City, Vietnam. 6.—Center for Innovative Materials and Architectures (INOMAR), Vietnam National University, Ho Chi Minh City, Vietnam. 7.—e-mail: yjcheng@ncnu.edu.tw. 8.—e-mail: pbthang@hcmus.edu.vn

Dielectric breakdown induced by Cu ion migration in porous low-*k* dielectric films has been investigated in alternating-polarity bias conditions using a metal–insulator–metal capacitor with Cu top metal electrode. The experimental results indicated that Cu ions migrated into the dielectric film under stress with positive polarity, leading to weaker dielectric strength and shorter time to failure (TTF). In the alternating-polarity test, the measured TTFs increased with decreasing stressing frequency, implying backward migration of Cu ions during reverse-bias stress. Additionally, compared with a direct-current stress condition, the measured TTFs were higher as the frequency was decreased to 10^{-2} Hz. The electric-field acceleration factor for porous low-*k* dielectric film breakdown in the alternating-polarity test was also found to increase. This Cu backward migration effect is effective when the stressing time under negative polarity is longer than 0.1 s.

Key words: Cu-induced dielectric breakdown, porous low-*k* dielectric films, alternating-current stress, direct-current stress, time to failure

INTRODUCTION

Porous low-*k* dielectric films with dielectric constant below 2.8 are widely used in ultralarge-scale integrated chips for technology nodes at 45 nm or below to reduce signal propagation delays, dynamic power consumption, and crosstalk noise.[1,2] However, such porous low-*k* dielectric films face serious reliability issues when integrated into advanced back-end-of-line (BEOL) interconnects because of their weaker dielectric strength and the higher electric fields sustained at continuously scaled-down geometric sizes.[3] Consequently, it is important to improve understanding on the breakdown failure physics of such porous low-*k* dielectric films. The breakdown characteristics of porous low-*k* dielectric films have been extensively investigated.[4–6] Most of these studies investigated static reliability, in which testing is usually performed under direct-current (DC) conditions. However, electronic devices are usually operated in alternating-current (AC) rather than DC mode in most real-world applications. The breakdown characteristics of porous low-*k* dielectric films in this regime have received little attention so far. Therefore, it is important to understand the dielectric breakdown characteristics of porous low-*k* dielectric films under AC stress.

On the other hand, Cu ion drift into the interlayer dielectric has been reported to be a major degradation factor affecting BEOL dielectric reliability.[7–11] Results reported under DC stress are similar to one another, indicating that low-*k* dielectric films have

(Received October 22, 2016; accepted January 26, 2017)

Published online: 10 February 2017

reduced dielectric breakdown time when Cu ions drift into the film.[7,8] On the contrary, results obtained under AC stress are contradictory.[9–11] Chen et al.[9] reported enhanced dielectric breakdown time under AC compared with DC stress, which was attributed to retardation of Cu ion migration in the dielectric when the voltage polarity was reversed. A similar result was reported by Jung et al.,[10] who also indicated that increasing the frequency of the AC stress resulted in longer dielectric breakdown time due to the inability to inject Cu ions into the dielectric at high frequency. On the other hand, Miyazaki et al.[11] found shorter dielectric failure time under AC compared with DC stress for Cu/low-*k* damascene structures. To address these discrepancies and understand the role of Cu ions in porous low-*k* dielectric breakdown under AC stress, bipolar AC stressing tests at various frequencies were performed on porous low-*k* dielectric films in this study. Metal–insulator–metal (MIM) capacitors with Cu metal as top electrode were fabricated and used to measure the dielectric breakdown time.

EXPERIMENTAL PROCEDURES

Porous low-*k* SiCOH dielectric films were deposited by plasma-enhanced chemical vapor deposition (PECVD) using diethoxymethylsilane (DEMS) and α-terpinene (ATRP) as matrix and porogen precursor, respectively. A small amount of oxygen was also introduced as oxidant. The deposition temperature, pressure, and power were 300°C, 1.0×10^4 Pa, and 600 W, respectively. After deposition, ultraviolet (UV) curing at wavelength of 200 nm to 450 nm at 350°C was performed for 300 s to remove the organic porogen and form micropores in the low-*k* film. The average pore size and porosity of the resulting porous low-*k* films were measured to be 1.4 nm and 15%, respectively, as determined from the isotherm of ethanol adsorption and desorption using ellipsometric porosimetry (Semilab, Mode PS-1100). The dielectric constant was determined to be 2.56 through capacitance–voltage measurements using a SSM Inc. Hg probe 5100 CV system at 1 MHz. The thickness of the resulting porous low-*k* dielectric films was 320 ± 20 nm, as analyzed using an ellipsometer in an optical probe system.

The porous low-*k* dielectric films were deposited on *n*-type silicon substrate or $TaN/SiO_2/Si$ stacked structure to fabricate metal–insulator–silicon (MIS) or MIM capacitors. To fabricate the $TaN/SiO_2/Si$ stacked structure, TaN and SiO_2 films were deposited sequentially on *n*-type silicon substrate, using physical vapor deposition and thermal oxidation methods, respectively. After deposition of the porous low-*k* dielectric film, metal film (Al or Cu) was deposited as a metal electrode on the top surface through a shadow mask by a thermal evaporation method. The thickness of the metal film was about 100 nm, and the formation area of the metal electrode was 9.0×10^{-4} cm^2. Figure 1 shows the structures of the fabricated MIS and MIM capacitors, which were used to measure the capacitance–voltage (*C*–*V*), current–voltage (*I*–*V*), and time-dependent dielectric breakdown (TDDB) characteristics under DC and AC stress. TDDB measurements were performed in fixed electric field to record the failure time, at which the monitored leakage current suddenly increases. *C*–*V* measurements were carried out at frequency of 1 MHz using a semiconductor parameter analyzer (HP4280A). *I*–*V* and TDDB measurements were performed using an electrometer (Keithley, 6517A). All measurements were performed at room temperature (25°C).

RESULTS AND DISCUSSION

Figure 2 plots the measured *C*–*V* characteristics of MIS and MIM structures with Cu or Al electrode. For the MIM structure, the measured capacitance remained constant for both positive and negative voltage. For both the MIS and MIM structures with identical Al electrode, the measured accumulation capacitances were similar. The measured accumulation capacitance of the MIS or MIM structure with Cu electrode was higher than that with Al electrode. Thus, the dielectric constants of the porous low-*k* dielectric films were calculated to be 2.58 ± 0.06 and 2.74 ± 0.10 for the Al and Cu electrode cases. The dielectric constant of the studied porous low-*k* dielectric film was measured to be 2.56 using a SSM Inc. Hg probe 5100 CV system, which is thought to be close to the real value with little impact from the deposition of the electrode. Therefore, it can be concluded that the dielectric constant of the porous low-*k* dielectric film was less impacted by the deposition of the Al electrode than the Cu electrode. This result also indicates that diffusion of Cu ions from the electrode into the porous low-*k* dielectric film was faster than that of Al ions. This can be explained by the fact that the Cu atom is larger (four orbits) than the Al atom (three orbits). Since the Cu atom has only one electron in the fourth orbit, it is much easier to ionize Cu atoms to form Cu^+ ions.[12] Migration of a large amount of Cu ions into the porous low-*k* dielectric film leads to a large increase in the dielectric constant. Additionally, for the MIS structure, *C*–*V* measurements were performed using a voltage sweep from inversion (positive voltage) to accumulation (negative voltage) and then back. As shown in Fig. 2, the *C*–*V* curves shifted significantly for the Cu electrode case but remained unchanged for the Al electrode case. Such a shift in *C*–*V* curves has been reported to originate from dielectric polarization, mobile ions, or formation of metal ions from the electrode.[13] In this study, the preparation method for the porous low-*k* dielectric film was identical, thus the first two effects (dielectric polarization and mobile ions) on the shift in the *C*–*V* curves were similar. Therefore, the difference in the shift of the *C*–*V* curves for the MIS

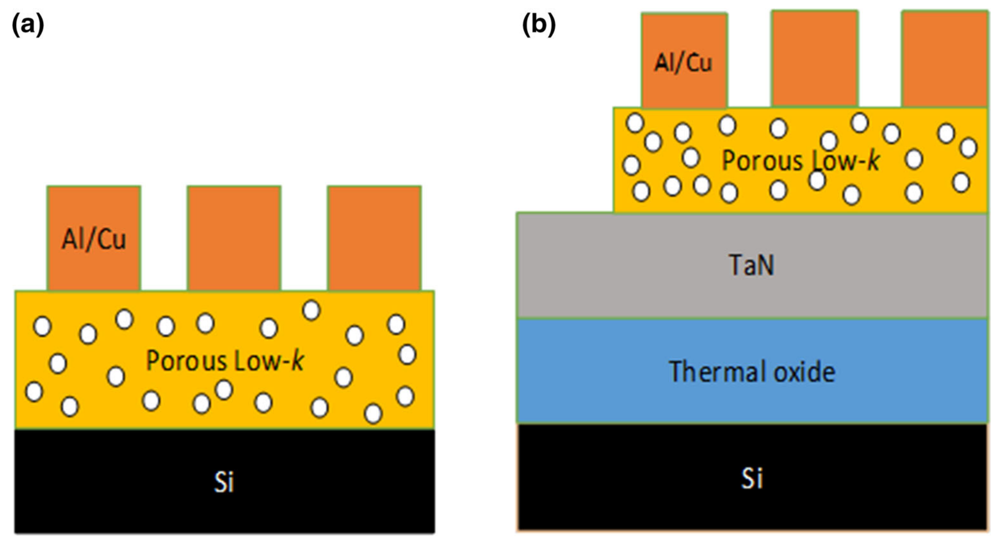

Fig. 1. Schematics of test structures employed in this study: (a) MIS and (b) MIM capacitor structures.

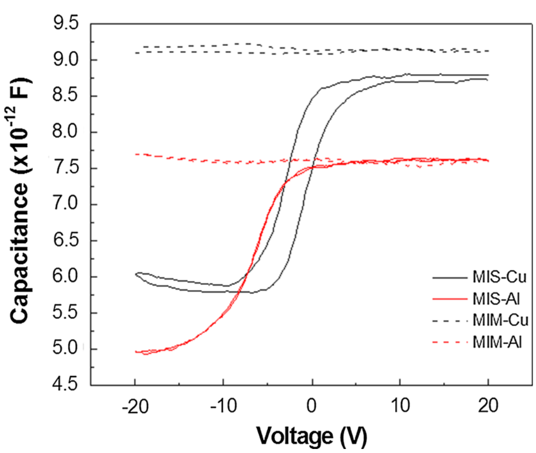

Fig. 2. *C–V* characteristics of MIS and MIM capacitors with Cu or Al electrode.

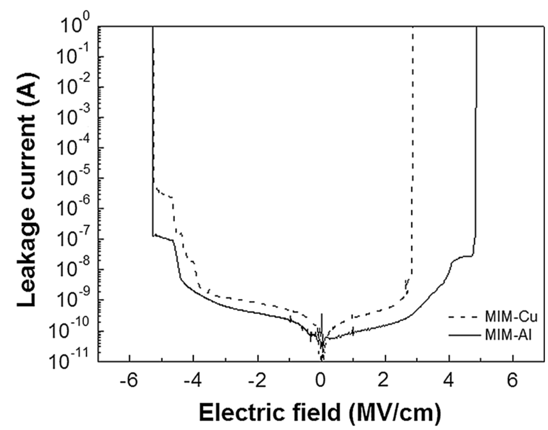

Fig. 3. *I–E* characteristics of MIM capacitors with Cu or Al electrode.

structures with Cu or Al electrode must result from metal ions from the electrode. The larger shift in the *C–V* curves for the MIS capacitors with Cu electrode again demonstrates that more Cu ions migrated into the porous low-*k* dielectric film.

Figure 3 presents the measured leakage current–electric field (*I–E*) plots of MIM capacitors with Cu or Al electrode under positive and negative polarity. For MIM capacitors with Al electrode under stressing with positive and negative polarity, the *I–E* behaviors were similar. The leakage current first increased with the stressing electric field for weak electric fields, then reached a plateau, before finally increasing abruptly by at least three orders of magnitude. The electric field at this jump is defined as the dielectric breakdown electric field. For MIM capacitors with Cu electrode under stressing with negative polarity, the *I–E* behavior was similar to that for MIM capacitors with Al electrode. However, under stressing with positive polarity, the leakage current increased with the stressing electric field without a plateau stage before dielectric breakdown. This suggests that the migration of Cu atoms into the porous low-*k* dielectric film showed different behaviors under stressing with positive versus negative polarity.

Figure 4 compares the dielectric breakdown electric field of the porous low-*k* dielectric films in the MIM capacitors with Al or Cu electrode. As presented, the measured dielectric breakdown strength was impacted by the metal electrode type and the stressing polarity. For both MIM capacitors with Al and Cu electrodes, the breakdown electric field of the porous dielectric film under stressing with positive polarity was lower than that under stressing with negative polarity, indicating that Al and Cu atoms were oxidized to form ions and an electric field was established across the dielectric film. Therefore, the formed ions moved along the direction of an electric field. Under stressing with

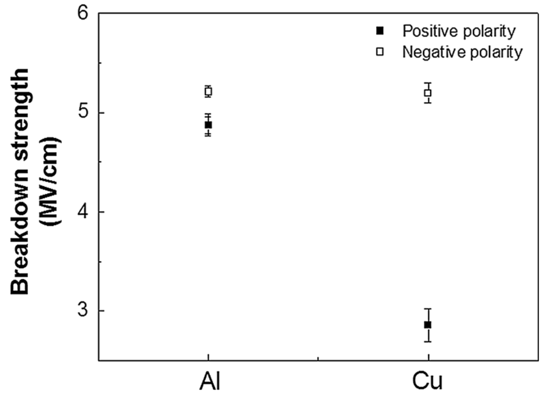

Fig. 4. Comparison of breakdown field for MIM capacitors with Cu and Al electrodes under positive and negative polarities.

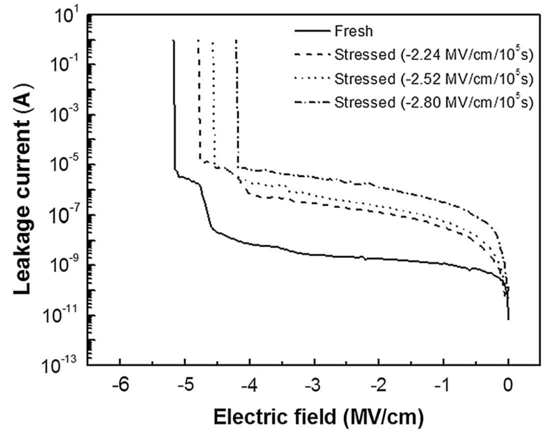

Fig. 5. Comparison of *I–E* characteristics of fresh and stressed MIM capacitors with Cu electrode under stress with negative polarity.

negative polarity, the breakdown electric fields of the porous low-*k* dielectric films in the MIM capacitors with Al and Cu electrodes were similar, suggesting that no metal ions were formed. Hence, the difference in the breakdown electric field with positive versus negative polarity was larger for the MIM capacitors with Cu electrode compared with the samples with Al electrode. The breakdown electric field of the porous low-*k* dielectric film in the MIM capacitors with Cu electrode was lower by about 2.2 MV/cm under stressing with positive compared with negative polarity, indicating that more Cu ions formed and were easily driven into the porous low-*k* dielectric film under stressing with positive polarity. In the case of the MIM capacitors with Al electrode, the difference in the dielectric breakdown electric field was only 0.4 MV/cm. This result indicates that Al ions can migrate into the porous low-*k* dielectric film under stressing with positive polarity, but this migration effect is not obvious relative to the Cu electrode.

To understand the effect of migration of Cu ions into the porous low-*k* dielectric film on its long-term dielectric reliability, TDDB tests under DC stress were performed on the MIM capacitors with Cu electrode. The stress voltages had either positive or negative polarity. The time to failure (TTF), or lifetime, is defined as the time at which the leakage current reaches a certain level (here, 10^{-3} A). For the applied stressing voltages with positive or negative polarity, the porous low-*k* dielectric film failed within 1.0×10^4 s under stressing with positive polarity for electric fields of 2.20 MV/cm to 2.80 MV/cm, while no failure event was detected under stressing with negative polarity even after stressing time of 1×10^5 s. This indicates that Cu ions are formed under stressing with positive polarity and then diffuse into the porous low-*k* dielectric film, accelerating the dielectric breakdown with shortened TTF. Although no failure occurred under stressing with negative polarity, it was observed that the leakage current started to increase gradually after a period of stressing time. The *I–E* characteristics of the MIM structures with Cu electrode that were stressed in negative electric fields of 2.2 MV/cm to 2.8 MV/cm for 10^5 s were measured, and the results are compared with fresh samples in Fig. 5. The MIM capacitors stressed with negative polarity displayed increased leakage current and reduced dielectric breakdown electric field compared with fresh samples. Moreover, the degradation in the electrical performance became more obvious with increasing applied electric field. Under stressing with negative polarity at 2.2 MV/cm, 2.5 MV/cm, and 2.8 MV/cm for 10^5 s, the leakage currents in an electric field of 2 MV/cm for MIM capacitors with porous low-*k* dielectric film increased from 1.79×10^{-9} A to 1.22×10^{-7} A, 2.23×10^{-7} A, and 1.28×10^{-6} A, respectively. The corresponding dielectric breakdown electric fields were reduced from 5.16 MV/cm to 4.76 MV/cm, 4.54 MV/cm, and 4.18 MV/cm. Although migration of Cu ions was not detected under stressing with negative polarity, trapped charges resulted in breakdown of the porous low-*k* dielectric film. This damage was relatively weak compared with that under stressing with positive polarity due to the lack of Cu-catalyzed dielectric breakdown (Fig. 6).

Under stressing with positive polarity, the TTF of the porous low-*k* dielectric films in the MIM capacitor with Cu metal electrode as a function of the applied electric field was measured and is plotted in Fig. 7. The TTFs of the porous low-*k* dielectric films were detected to decrease with increasing applied electric field. This implies that more Cu ions formed and migrated into the porous low-*k* dielectric film under stressing with positive polarity at higher electric field, accelerating dielectric breakdown. Additionally, the variation of the measured TTFs was larger for higher stressing electric field. It is believed that, in addition to stronger electric damage to the low-*k* dielectric film, the diffusion of Cu ions into the porous low-*k* dielectric film became more intense for higher stressing electric field. Both damage mechanisms to the low-*k* dielectric film

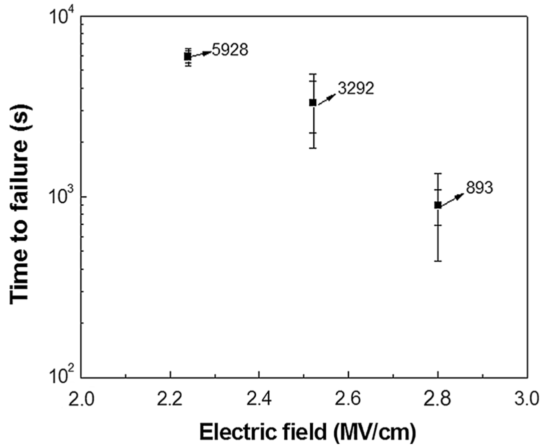

Fig. 6. TTF of MIM capacitors with Cu electrode under DC stress with positive polarity as function of electric field.

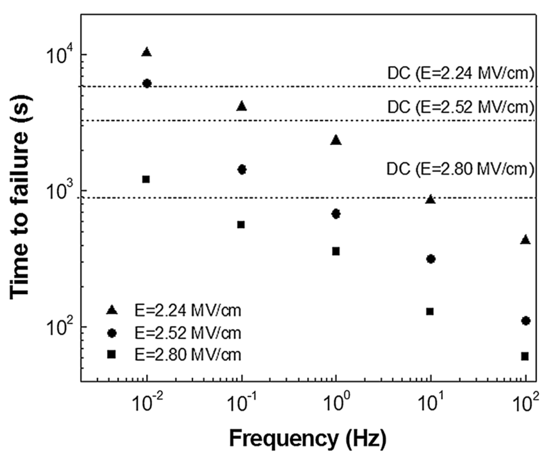

Fig. 7. TTFs of MIM capacitors with Cu electrode under bipolar AC stresses as function of frequency.

induced a larger variation in the TTF. Furthermore, an E model with TTF $\sim \exp(-\gamma E)$ was applied to describe the electric field dependence of the dielectric breakdown behavior.[14,15] This model contains an important parameter, i.e., the electric-field acceleration factor (γ), which represents the degree of influence of the applied electric field on the dielectric failure time. The obtained value of the electric-field acceleration parameter was 3.52, lower than reported values obtained from Al-electrode structures.[16] This result indicates that Cu ion migration-induced low-*k* dielectric breakdown leads to a decreased electric-field acceleration parameter. Hence, the dielectric breakdown time of porous low-*k* dielectric film is less impacted by the applied electric field because of the presence of the Cu ion-catalyzed breakdown mechanism. With such a lower electric-field acceleration parameter, the lifetime in a lower operation field is predicted to be worse.

Alternating-polarity TDDB tests were also performed on MIM capacitors with Cu electrode. The frequency of the bipolar AC stress was varied from 10^{-2} Hz to 10^{2} Hz, while the duty cycle was kept at 50%. The TTF under bipolar AC stress only counted the stressing time with positive polarity. According to the results obtained under DC stress conditions, dielectric degradation due to electric stressing occurred in stress with either positive or negative polarity. Under stress with positive polarity, another dielectric degradation mechanism (drift of Cu ions into the dielectric film) was detected, significantly accelerating the occurrence of dielectric breakdown. Furthermore, under bipolar AC stress, the breakdown characteristics became complex due to the Cu ion recovery effect in reversed polarity. If Cu ion drift is reversible under negative polarity, the porous low-*k* dielectric film tested under bipolar AC stress should exhibit longer TTF than under DC stress with positive polarity. However, the fold increase depends on the degree of Cu ion recovery. On the other hand, if Cu ion drift is a nonreversible mechanism, bipolar AC stress would create either two independent breakdown paths or an overlay breakdown path from both sides of the dielectric. If the former occurs, the failure time under bipolar AC stress should be equal to or less than the dielectric failure time measured under DC stress with positive polarity. However, if the latter occurs, the failure time under bipolar AC stress should be lower. Figure 7 compares the average TTFs of the porous low-*k* dielectric films measured at five sites under bipolar AC stress with different electric fields as a function of the stressing frequency. In fixed electric field, the TTFs of the porous low-*k* dielectric film increased with decreasing frequency under bipolar AC stress. This suggests that the Cu ions can be recovered back from the low-*k* dielectric film during stressing with negative polarity and that this recovery effect becomes particularly stronger at lower stressing frequency. This may also imply that a certain time is needed to trigger the occurrence of Cu ion recovery. When the porous low-*k* dielectric films were stressed under bipolar AC stress at higher frequency, the stressing time under negative polarity was insufficient to drive Cu ions back from the low-*k* dielectric film. Thus, a lower TTF was detected. This suggestion is also supported by the observation that the variations of the measured TTFs were larger under bipolar AC stress at lower frequency, because another mechanism of Cu ion recovery participated in the dielectric breakdown. Additionally, the TTFs measured under AC stress exceeded those under DC stress when the stressing frequency was decreased to a certain value. For all electric fields from 2.24 MV/cm to 2.80 MV/cm, this frequency was constant at 10^{-2} Hz. However, the increased folds were 1.49, 1.88, and 1.30 under stressing electric fields of 2.24 MV/cm, 2.52 MV/cm, and 2.8 MV/cm, respectively. The optimized improvement in electric field of 2.52 MV/cm implies that the recovery of Cu ions back from the low-*k* dielectric film is more efficient in this applied field. Higher or lower

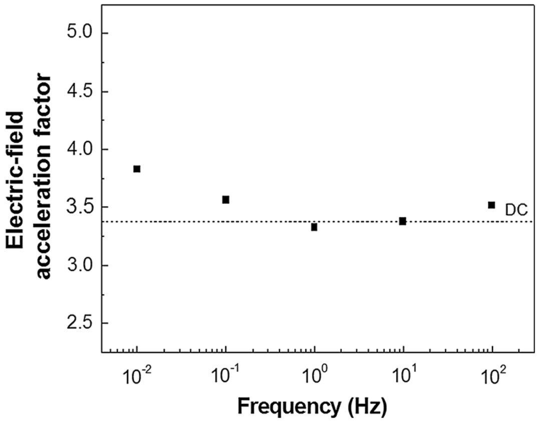

Fig. 8. Electric-field acceleration parameter of MIM capacitors with Cu electrode under bipolar AC stress as function of frequency.

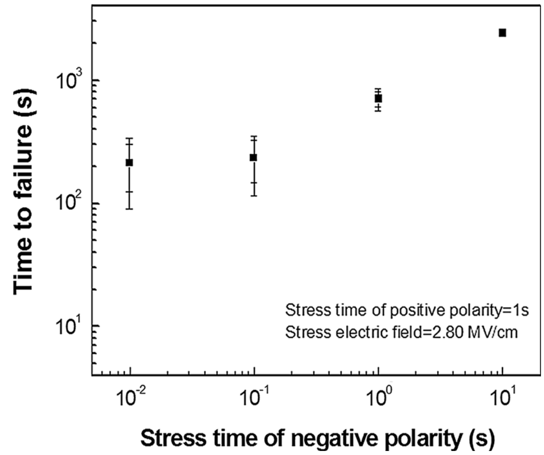

Fig. 9. TTFs of MIM capacitors with Cu electrode under bipolar AC stress as function of stressing time with negative polarity (stressing time in positive polarity = 1 s).

electric fields could not recover all the diffused Cu ions back to the electrode from the porous low-*k* dielectric film.

Under AC stress at different frequencies, the electric-field acceleration parameter was also extracted using the E-model and is presented in Fig. 8. The results for DC stress are also listed for reference. As shown, the electric-field acceleration parameter obtained under AC stress depended on the stressing frequency. When the stressing frequency was larger than 1 Hz, the obtained electric-field acceleration parameters were similar to those obtained under DC stress. When the stressing frequency was lower than 1 Hz, the obtained electric-field acceleration parameters were higher than those obtained under DC stress and increased with decreasing stressing frequency. This suggests that the Cu recovery effect leads to an increased electric-field acceleration parameter. Under AC stress with stressing frequency of 10^{-2} Hz, the largest electric-field acceleration parameter of 3.83 was obtained, indicating the best Cu ion recovery effect. On the other hand, the electric-field acceleration parameter obtained under AC stress with stressing frequency above 1 Hz was similar to that obtained under DC stress, indicating an inefficient Cu ion recovery effect.

Under alternating-polarity bias stress, recovery of Cu ions back from the low-*k* dielectric film is believed to occur during the stress with negative polarity. Through this backward Cu ion migration effect, the dielectric breakdown time can be prolonged. To further understand the effectiveness of Cu ion recovery, alternating-polarity TDDB tests were performed. The stressing time with positive polarity was fixed at 1 s, while the stressing time with negative polarity was varied, ranging from 10^{-1} s to 10 s. The stressing electric field in both positive and negative polarities was kept at 2.8 MV/cm. The obtained TTF only counted the stressing time with positive polarity. Figure 9 plots the measured TTFs as a function of stressing time with negative polarity, clearly showing that the dielectric breakdown time remained constant when the stressing time with negative polarity was shorter than 10^{-1} s, then increased with the stressing time with negative polarity, indicating a critical time to enhance the dielectric breakdown time due to the Cu ion recovery effect. This critical time (herein 10^{-1} s) is presumed to be the time required for Cu ion recovery from the dielectric film to the gate electrode. Stressing time with negative polarity below 10^{-1} s is insufficient to drive the Cu ions back to the gate electrode. Therefore, the Cu ion recovery effect becomes negligible, leading to no enhancement of the dielectric breakdown time.

CONCLUSIONS

The effect of Cu ion migration on the breakdown characteristics of porous low-*k* dielectric film was studied using alternating-polarity TDDB tests. Under stress with positive polarity, porous low-*k* dielectric films exhibited weaker dielectric strength and shorter TTF due to migration of Cu ions into the film. When alternating-polarity bias stress was applied, the measured TTF increased with decreasing stressing frequency, indicating stronger backward migration of Cu ions during the reverse-bias stress at lower frequency. Furthermore, this Cu backward migration effect is effective when the stressing time with negative polarity is longer than 0.1 s. When the frequency in the alternating-polarity test was decreased to 10^{-2} Hz, the measured TTFs were longer than those under the DC stress condition.

ACKNOWLEDGEMENTS

The authors would like to thank the National Science Council of the Republic of China, Taiwan, for supporting this research financially under Contract No. MOST-103-2221-E-260-009.

REFERENCES

1. A. Grill, *Annu. Rev. Mater. Res.* 39, 49 (2009).
2. C.K. Choi, H.S. Lee, R. Navamathavan, J.K. Woo, and C.Y. Kim, *Thin Solid Films* 78, 6474 (2010).
3. J. Yuan, C. Ye, Z. Xing, Y. Xu, and Z. Ning, *Microelectron. Eng.* 86, 2119 (2009).
4. F. Chen and M.A. Shinosky, *Microelectron. Reliab.* 54, 529 (2014).
5. I. Fisher and M. Eizenberg, *Thin Solid Films* 516, 4111 (2008).
6. B.J. Tang, K. Croes, Y. Barbarin, Y.Q. Wang, R. Degraeve, Y. Li, M. Toledano-Luque, T. Kauerauf, J. Bommels, Zs. Tokei, and I. De Wolf, *Microelectron. Reliab.* 54, 1675 (2014).
7. F. Chen, O. Bravo, D. Harmon, M. Shinosky, and J. Aitken, *Microelectron. Reliab.* 48, 1375 (2008).
8. P. Belsky, R. Streiter, H. Wolf, S.E. Schulz, O. Aubel, and T. Gessner, *Microelectron. Eng.* 92, 107 (2012).
9. F. Chen, O. Bravo, K. Chanda, P. Mclaughlin, T. Sullivan, J. Gill, J. Lioyd, R. Kontra, and J. Aitken, in *Proceedings of International Reliability Physics Symposium* (2006), pp. 46–53.
10. S.Y. Jung, B.J. Kim, N.Y. Lee, B.M. Kim, S.J. Yeom, N.J. Kwak, and Y.C. Joo, *Microelectron. Eng.* 89, 58 (2012).
11. H. Miyazaki, D. Kodama, and N. Suzumura, in *Proceedings of International Reliability Physics Symposium* (2008), pp. 150–157.
12. K.C. Aw and K. Ibrahim, *Thin Solid Films* 434, 178 (2003).
13. B.Y. Tsui, K.L. Fang, and S.D. Lee, *IEEE Trans. Electron Dev.* 48, 2375 (2001).
14. H. Cui, I.B. Bhat, S.P. Murarka, H. Lu, W.J. Hsia, and W. Catabay, *J. Vac. Sci. Technol. B* 20, 1987 (1997).
15. J.W. McPherson, *Microelectron. Reliab.* 52, 1753 (2012).
16. E.T. Ogawa, J. Kim, G.S. Haase, H.C. Mogul, and J.W. McPherson, in *Proceedings of International Reliability Physics Symposium* (2012), pp. 166–172.